ACS Pharmacology & Translational Science

pubs.acs.org/ptsci Article

Phenolic Preservative Removal from Commercial Insulin Formulations Reduces Tissue Inflammation while Maintaining Euglycemia

Adam Mulka, Brianne E. Lewis, Li Mao, Roshanak Sharafieh, Shereen Kesserwan, Rong Wu, Donald L. Kreutzer, and Ulrike Klueh*

Cite This: *ACS Pharmacol. Transl. Sci.* 2021, 4, 1161−1174 Read Online

ACCESS | Metrics & More | Article Recommendations | Supporting Information

ABSTRACT: Background: Exogenous insulin therapy requires stabilization of the insulin molecule, which is achieved through the use of excipients (e.g., phenolic preservatives (PP)) that provide protein stability, sterility and prolong insulin shelf life. However, our laboratory recently reported that PP, (e.g., *m*-creosol and phenol) are also cytotoxic, inducing inflammation and fibrosis. Optimizing PP levels through filtration would balance the need for insulin preservation with PP-induced inflammation. **Method**: Zeolite Y (Z-Y), a size-exclusion-based resin, was employed to remove PP from commercial insulin formulations (Humalog) before infusion. **Results**: PP removal significantly decreased cell toxicity *in vitro* and inflammation *in vivo*. Infusion site histological analysis after a 3 day study demonstrated that leukocyte accumulation increased with nonfiltered preparations but decreased after filtration. Additional studies demonstrated that a Z-Y fabricated filter effectively removed excess PP such that the filtered insulin solution achieved equivalent glycemic control in diabetic mice when compared to nonfiltered insulin. **Conclusion**: This approach represents the proof of concept that using Z-Y for in-line PP removal assists in lowering inflammation at the site of insulin infusion and thus could lead to extending the functional lifespan of insulin infusion sets *in vivo*.

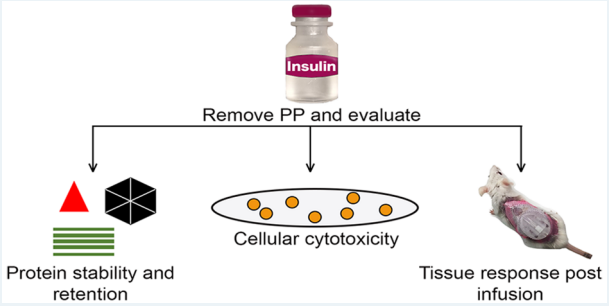

KEYWORDS: *insulin infusion pump, inflammation, insulin preservatives, zeolite, phenolic preservatives, continuous subcutaneous insulin infusion*

Diabetes mellitus (DM) should be considered a domestic epidemic in that cases will increase by 54% from approximately 35 million people today to nearly 55 million people by decade's end.[1] Globally, DM is predicted to affect more than 642 million people in this same interval.[1] Currently, the American Diabetes Association estimates that 7.5 million Americans are insulin-dependent and thus require frequent subcutaneous insulin administration (SIA) for glycemic control. Insulin usage site effects are common and can include skin irritation, inflammation, and scarring as a consequence of skin puncture and subsequent SIA and continuous subcutaneous insulin infusion (CSII).[2−8] While tissue site reactions are undoubtedly a limitation for many insulin users, they can be minimized when adhering to ADA guidelines on utilizing a stringent device site rotation regiment across multiple skin sites (e.g., buttocks, abdomen, and arms).[9−11] Lipohypertrophy (LH), an accumulation of excess adipose tissue under the skin, remains a common complication in the insulin-treated diabetes patient and is associated with an impaired absorption of insulin.[12−15] Poor injection technique as it relates to injection site rotation,[16] injection angle,[17] and repeated needle use are believed to be causative variables.[15] Although the anabolic effect of insulin on adipose tissue is appreciated,[18,19] investigations are warranted for the role of phenolic preservatives on fatty tissue and LH occurrence.

Significant progress in SIA and CSII technology has been realized over the past two decades.[20−26] I-Port Advance, as distributed by Medtronic, allows for repeated injections into the same port without the need for repetitive skin punctures. Emerging new technology in insulin delivery, such as distribution by Omnipod, or those in development (e.g., Tandem mini pump and EoPatch), are tubeless insulin pump systems which utilize sophisticated algorithms for precise insulin delivery. Insulin infusion pumps combined with new continuous glucose-sensing devices used in a closed-loop artificial pancreas have shown a greater duration of

Received: February 4, 2021
Published: April 26, 2021

https://doi.org/10.1021/acsptsci.1c00047
ACS Pharmacol. Transl. Sci. 2021, 4, 1161−1174

euglycemia.[27] Notwithstanding these advances, only a minority of insulin-dependent diabetes patients achieve optimal glucose control.[28,29] Currently, only rapid- or short-acting insulin formulations are utilized in infusion pumps.[5,30,31] All insulin formulations contain significant amounts (2.3−3.2 mg/mL) of phenolic preservatives (PP), namely, phenol and/or *m*-cresol, which are necessary in insulin formulations to stabilize insulin, allow for an extended shelf life, and provide sterility to the formulation.[32,33] Weber et al. reported that phenol and *m*-cresol induce cell death in vitro.[34] Both compounds manifested cytotoxicity at levels significantly less than employed in current clinical applications.[34] Subsequently, our laboratory demonstrated by using our murine air-pouch model that leukocytes, specifically neutrophils and monocytes/macrophages, serve a critical role in the tissue reactions observed at the sites of insulin and PP infusion.[35] Specifically, PP-containing infusions showed significant increases in total inflammatory cell influx, 3−5 times that of saline.[35] This data supports the hypothesis that PP induces a profound acute inflammatory response *in vivo*, which could compromise maintaining euglycemia and cause permanent destruction of the infusion site (i.e., fibrosis). Noticeably, investigating methodologies that would attenuate the inflammatory response could potentially extend the useful lifespan of CSII devices. It is well-established that removal of PP from the insulin solution can lead to protein aggregation.[32,33,36,37] Thus, we further hypothesize that development of real-time in-line devices that can remove PP immediately prior to insulin infusion *in vivo* would maintain insulin stability during storage while minimizing PP toxicity and inflammation during infusion, thus ensuring effective blood glucose control *in vivo*. Despite convincing data demonstrating the chemotoxicity of PP used in insulin formulations,[34,35] Swinney et al. recently reported that insulin itself and not the insulin phenolic preservatives are responsible for inflammation at the site of infusion pump sets.[38] In these studies, regular insulin with and without 2.5 mg/mL *m*-cresol was infused into subcutaneous swine tissue for up to 10 days. Subsequently, the tissue responses to these agents were compared. The authors concluded that since similar tissue reactions were observed at 10 days post-infusion that insulin itself was causative. However, this study did not consider confounding variables. Specifically, these authors did not investigate infusing the preservative alone, did not evaluate the tissue reaction at an early time with comprehensive tissue analyses, and omitted assessing for possible insulin aggregation without the presence of PP. Specifically, the formation of insulin aggregates will most likely exacerbate the tissue reaction at the infusion site.[39−41] Current challenges to extending the lifespan of infusion pump sets involve surmounting the foreign body reaction (FBR). FBR is an inflammatory response stimulated by the host's immune response to an external irritant. Cumulatively, the catheter material, shape, size, insulin aggregates/amyloids, and the infused preservative in an insulin formulation could all contribute to the FBR. Other challenges include the exposed wound, the catheter insertion device, the catheter's needle, and perhaps the catheter insertion angle.[42−44] FBR at an insulin device location cumulatively contributes to local skin irritation due to leukocyte recruitment and activation of the inflammatory cascade. Independent of the initiating source(s) of inflammatory cell recruitment, accumulation of leukocytes and associated proteases at insulin infusion sites could lead to increased insulin uptake and/or insulin degradation by inflammatory cells leading to an exacerbation of the inflammatory response and ultimately altering insulin absorption and blood glucose control. Identifying the targets triggering inflammation is critical to extending the longevity of insulin infusion sets. We opine that there are several major obstacles in achieving infusion set longevity with one being the chemotoxicity of the insulin solution containing PP.[35,45] Thus, our present study assessed the role of PP in the initiation of an inflammatory response. Consequently, our emphasis was directed at identifying strategies and prototype devices for PP removal immediately prior to tissue site infusion. Our study was designed to determine if reduced PP in insulin infusion is beneficial to minimizing tissue toxicity and inflammation, while maintaining insulin protein stability and activity.

Thus, this study endeavored to identify a mechanism for PP removal to minimize inflammation while maintaining protein stability and activity. We developed an efficient method of excipient removal by filtration immediately before insulin infusion using zeolites, based on previous studies by Eriksson.[46] Zeolites are a type of porous aluminosilicate used commercially for their adsorptive and catalytic capabilities. Zeolites are utilized in numerous applications ranging from petrochemical processing to medical devices for concentrating oxygen.[46−48] The porous structure of zeolite makes it an ideal filter material for size-exclusion filtration by trapping small components in the pores and allowing larger components to pass. Specifically, this study investigated the filtration efficiency of two types of zeolite, mordenite and zeolite Y, with further validation to determine protein adsorption in filtration materials and spectroscopic analysis monitoring protein structure. This investigation also evaluated the effects of filtration on insulin *in vivo* using a modified murine air-pouch model, which delivers a predictable infusion site permitting the evaluation of insulin absorption and activity.

MATERIALS AND METHODS

Cell Types Used for In Vitro Studies. Macrophage cells (RAW 264.7; mouse), embryonic fibroblasts (3T3-L1; mouse), and fat cells were derived from embryonic fibroblasts (3T3-L1; mouse) using methylisobutylxanthine, dexamethasone, and an "insulin cocktail" as described by Madsen et al.[49] Murine bone-marrow-derived mast cells (BMMC) were isolated and derived from C57BL/6j mice (Jackson Laboratory, Bar Harbor, ME) as previously described by Klueh et al.[50] THP-1 human monocytes cell lines (ATCC TIB-202) were obtained from ATCC Bioproducts (Manassas, VA). Human mast cells (HMC-1.2) were acquired from Millipore (Burlington, MA). All cell lines were cultured according to suppliers' instructions.

Peripheral Blood Mononuclear Cells Isolation. Human peripheral blood mononuclear cells (PBMC) were isolated from heparinized blood obtained from healthy donors via informed consent following the manufacturer's Histopaque-1077 (Sigma-Aldrich, St. Louis, MO) protocol and Wayne State University Institutional Review Board (IRB) regulations. Briefly, heparinized blood was diluted at a ratio of 1:1 with Histopaque-1077 and gently mixed prior to centrifugation at 400*g* for 30 min at room temperature. Next, the PBMC-containing middle layer was removed and suspended using PBS. Cells were centrifuged at 250*g* for 10 min prior to plating the cells at a concentration of 2.5×10^5 cells/plate in a 48-well plate for use in MTT cytotoxicity assay.

***In Vitro* Cytotoxicity Assay.** Metabolic cytotoxicity was measured via MTT assay (ATCC bioproducts Manassas, VA)

https://doi.org/10.1021/acsptsci.1c00047
ACS Pharmacol. Transl. Sci. 2021, 4, 1161−1174

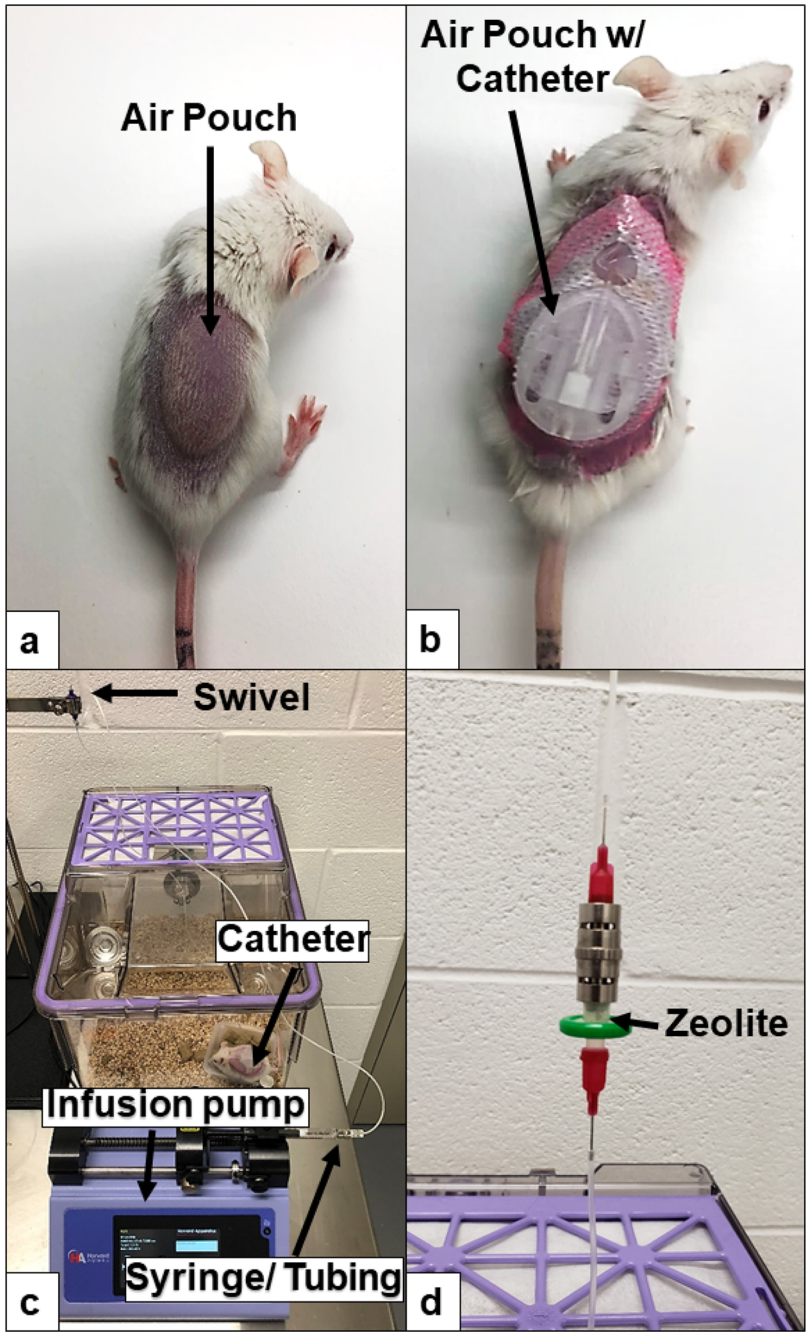

Figure 1. Mouse infusion setup: air-pouch infusion set up. (a) Air pouch prior to catheter insertion. (b) Air pouch with catheter. (c) Overview of our infusion setup including pump and integral swivel component. (d) Close up of in-line zeolite filter.

according to the manufacturer guidelines. Briefly, plated cells were incubated overnight in 250 μL of respective culture medium containing 10% fetal bovine serum (FBS) and 1% penicillin–streptomycin, without phenol red. Sterile diluent (Eli Lilly, Indianapolis, IN) with phenol and *m*-cresol concentrations of 0.65 and 1.60 mg/mL, respectively, and Humalog (Eli Lilly) were added at a serial dilution of 1:3. Following an incubation period of 1 or 3 days, the MTT reagent was added to the cells and incubated for a minimum of 1 h. Following incubation, supernatant was removed and replaced with dimethyl sulfoxide (Thermo Fisher, Waltham, MA) to dissolve the MTT reagent. Aliquots from each well were plated in a 96-well plate in duplicates and read at absorbance of 570 nm for analysis.

Zeolite Preparation. Zeolite preparation was modified from the protocol outlined by Eriksson.[46] Briefly, zeolite Y and mordenite (Tosoh Corporation, Tokyo, Japan) were heated at 250 °C for 30 min prior to dextran coating (MW 40 000; Alfa Aesar, Ward Hill, MA) to ensure pyrogen free compounds. To achieve proper dextran coating, dextran and zeolite Y were mixed 20:1 in PBS, respectively, and subsequently incubated at room temperature and 60 rpm for a minimum of 20 min. Next, the solution was centrifuged at 500*g* for 6 min, and the precipitate was washed with PBS. This step was repeated five times prior to resuspension in distilled water and drying overnight at 60 °C.

Phenolic Preservative Filtration. For filtration *in vitro*, 20 mg of zeolite was used to filter 1 mL of diluent or Humalog

https://doi.org/10.1021/acsptsci.1c00047
ACS Pharmacol. Transl. Sci. 2021, 4, 1161−1174

insulin using a 1 mL syringe and a 0.2 μm syringe filter. Diluent is commercially available from Eli Lilly and was used in our studies representing insulin preservatives.[35] Diluent has a combined PP concentration of 2.25 mg/mL with 1.60 mg/mL *m*-cresol and 0.65 mg/mL phenol. *In vivo* insulin infusion for mouse studies was performed with an in-line lab-made filter system. Components included a 0.2 μm syringe filter, a male luer adapter, and two 25 g blunt-tip needles. Zeolite (20 mg) was loaded into the syringe filter and luer-locked to the male luer adapter (depicted in Figure 1d).

Zeolite Adsorption Analysis Using HPLC. Adsorption measurements were derived from the protocol outlined by Eriksson with modifications.[46] Stock solutions of 3.5 mg/mL *m*-cresol and 2.0 mg/mL phenol (Fisher, Hanover Park, IL) were added to increasing amounts of zeolite (5−80 mg/mL) and vortexed for at least 15 s. Zeolite aliquots were separated from the solution through centrifugation at 4000 rpm for 5 min. Following centrifugation equal amounts of MeOH for HPLC analysis were added. HPLC was performed to determine phenolic adsorption and insulin retention. Phenolic adsorption was measured with a Waters 2685/996 PDA series HPLC system with a SynChropack C18 column (5 μm, 4.6 mm × 250 mm). The mobile phase flow rate was set to 1 mL/min. For each sample, 10 μL was injected by an autosampler. Mobile phase A utilized water containing 0.1% formic acid, whereas phase B employed methanol (MeOH). Solvent starting conditions were 0−1.5 min at 50% A and 50% B. After 1.5 min, the conditions were 30% A and 70% B for 6.5 min. The detection wavelength was 272.4 nm as determined from previous trial runs of analytes. *m*-Cresol and phenol standards for HPLC were purchased from SPEX CertiPrep (Metuchen, NJ) for calibration. Calibration equations were generated using linear regression. Eight samples of each *m*-cresol and phenol at 1 ppm were used to evaluate limits of detection (LOD). On the basis of ICH guidelines, LOD was determined by the mean area of the signal plus 3 standard deviations over the slope of the calibration line, whereas the limit of quantification (LOQ) was determined by the mean of the signal area plus 10 standard deviations over the slope of calibration line.[51] When plotted against the calibration curve, the LOQ was 2.7 ppm. Protein adsorption following filtration was determined (20 mg of zeolite/1 mL of Humalog) using a Waters 125 Å X-bridge SEC column pre-equilibrated with mobile phase (10 mM TRIS HCl, 140 mM NaCl, pH 7.5. degassed and 0.2 μM filtered) set to 1 mL/min.[52] Absorbance was measured at 215 nm, and spectra were collected on 3 independent samples.

Pressure Measurement of In-Line Zeolite Filters. Pressure changes in-line were measured using a PressureMAT pressure monitoring system and PRESS-S-000 pressure sensor (Pendotech, Princeton, NJ), used in conjunction with an Animas OneTouch Ping (West Chester, PA) and in-house in-line zeolite filters (Figure 1 d). Testing was carried out at basal infusion rate of 0.5 U/h.

Circular Dichroism of Humalog Protein. Circular dichroism (CD) was used to characterize the secondary structure and oligomeric state of Humalog because of filtration through the dextran-coated zeolite. An average of 10 scans were collected from 3 different lots of Humalog. Data was collected on a Jasco 1500 CD spectrophotometer under nitrogen from 400−250 nm at 50 nm/min in a 1 mm quartz cuvette (near-UV) and 250−200 at 20 nm/min in a 0.01 mm quartz cuvette (far-UV). Scans were accumulated and buffer-subtracted to reduce the signal-to-noise ratio. Excipients in Humalog contributed to noise in the 265−285 nm region despite background subtraction. Data presented below represent the average of all samples and scans (error bars are not presented for clarity). Humalog protein was scanned first, then filtered through Z-Y and scanned immediately after.

Mice. Hsd:ICR (CD-1) mice were purchased from Envigo (Somerset, NJ) or maintained at in-house facilities. Mice used in these studies had an average weight between 30−40 g. All studies were conducted with approval from the institutional animal care and use committee (IACUC) at Wayne State University.

Streptozotocin Induction of Diabetes in CD-1 Mice. Diabetes was induced following the protocol developed by Wu et al.[53] Briefly, male mice received daily intraperitoneal injections of streptozotocin (STZ) (50 mg STZ/kg body weight) for 5 days (Sigma-Aldrich, St. Louis, MO). STZ was prepared by dissolving 50 mg of STZ in 100 mM sodium citrate buffer (pH 4.5) and immediately injected following the preparation. Blood glucose levels were monitored at least twice weekly following STZ treatment using a Bayer Contour Next EZ Meter (Ascensia Diabetes Care, Parsippany, NJ). Mice with a blood glucose level above 250 mg/dL for two sequential blood glucose tests were designated as diabetic.

Murine Air-Pouch Model and Infusion Systems. The classic murine air-pouch model was adapted to evaluate the tissue response to infused agents.[35] Briefly, a total of 3 mL of filtered air (Millipore, 0.22 μm) was injected subcutaneously (s.c.) into the shaved back of female CD-1 mice and male STZ-induced diabetic mice, creating a sustained compartment (pouch) (Figure 1 a). Following air-pouch generation, infusion set cannulas are implanted into the air pouch while mice were anesthetized (Animas Inset 30 Infusion System, ADW Diabetes, Pompano Beach, FL) (Figure 1 b). An infusion rate of 50 μL/h was maintained continuously for the duration of each study utilizing infusion-only pumps obtained from Harvard Apparatus (Holliston, MA), and 1000 series gastight infusion syringes were obtained from Fisher Scientific (Waltham, MA) (Figure 1c). In-line zeolite filters were utilized to remove excipients from the insulin just prior to infusion (Figure 1d). Saline, diluent (sterile diluent for Humalog, Eli Lilly & Co., Indianapolis, IN), and Humalog insulin were infused at a continuous rate of 50 μL/hour for 3 days in STZ-induced diabetic mice. The continuous rate was based on a delivery rate of 25 uL/h, which approximates an average 60 U per day including insulin boluses.[54] This infusion rate was doubled to account for additional surface area in the air-pouch model. Humalog U100 was diluted in sterile diluent from Eli Lilly. The concentration of the Humalog was varied between 0.25−2 U/100 μL depending on the diabetic mice blood glucose (BG) levels to maintain blood glucose levels as close to euglycemia as possible. BG levels were monitored using a Bayer Contour Next EZ Meter (Ascensia Diabetes Care, Parsippany, NJ).

Leukocyte Isolation from Air Pouch. Mice were sacrificed 72 h after the infusion's initiation. The air pouch was lavaged using 10 mL of 0.9% saline (Baxter, Deerfield, IL) for cell fluid collection. The collected cell fluid was centrifuged at 1000 rpm for 5 min. The cells were washed twice with 10 mL of a 2% fetal bovine serum (Atlanta Biologicals, Flowery Branch, GA) in phosphate-buffered saline (Fisher Scientific, Waltham, MA)).

https://doi.org/10.1021/acsptsci.1c00047
ACS Pharmacol. Transl. Sci. 2021, 4, 1161−1174

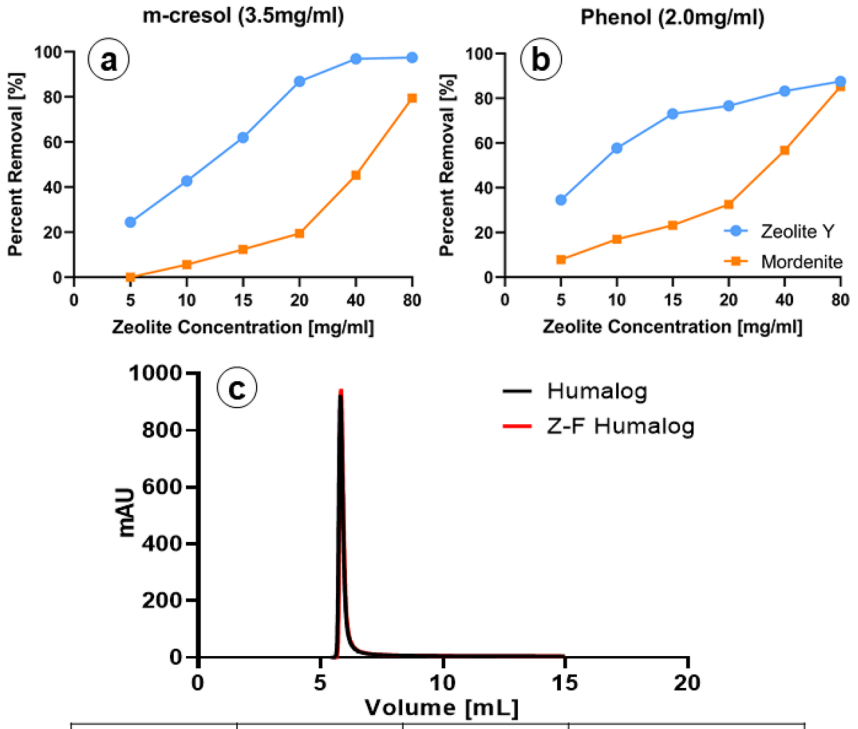

	Elution Time	Peak Area	Filtration Recovery
Humalog	5.80 ± 0.03	211.8 ± 1.25	-
Z-F Humalog	5.82 ± 0.02	207.1 ± 2.35	97.8% ± 0.6

Figure 2. Zeolite filtration of phenols: (a and b) Evaluation of both Z-Y and mordenite show that both types of zeolite are capable of filtering *m*-cresol and phenol from solutions containing either *m*-cresol or phenol (n = 2, triplicate measurements). Z-Y shows a higher overall affinity for *m*-cresol and phenol than does mordenite at all concentrations (error bars too small to display. All SD < 1%). (c) Z-Y coated with dextran showed negligible amounts of insulin adsorption to the material. Error values represent standard deviation (n = 3, triplicate measurements).

Flow Assisted Cell Sorting (FACS) Analysis. Air-pouch leukocyte populations were identified through flow cytometry, as previously conducted in our laboratory.[35] FACS analyses were performed on a BD LSR II utilizing the services of the microscopy, imaging, and cytometry core laboratory (MICR), at Wayne State University, Detroit, MI, and data were analyzed with FlowJo software (FlowJo, LLC).

Histological Evaluation. To evaluate tissue responses in each respective animal model after infusions, qualitative histopathologic evaluation was performed.[35] Mouse tissue was evaluated 3 days post-infusion. Mice were euthanized, the air pouch was lavaged, and the tissue was removed and fixed in 10% buffered formalin (VWR, Radnor, PA) for 24 h, followed by standard tissue preparatory steps, embedded in paraffin, and sectioned.[35] Tissue samples were cut into 5 μm sections and stained using standard hematoxylin and eosin stain (H&E) as well as anti-mouse CD31 (Abcam, cat: ab28364) and anti-mouse F4/80 (Fisher Scientific, cat: MF48000) antibody stains. Tissue samples were cut into 5 μm sections and H&E stained. Tissue samples were evaluated using a Nikon microscope and imaging system.

Statistical Analysis. All analyses were conducted using SAS version 9.4 (SAS, Inc., Cary, NC). A two-tailed *t*-test was performed to assess for statistical significance at an alpha of 0.05. *In vitro* data sets were analyzed by two-way ANOVA for multiple comparisons. Following FACS staining and analysis of the cell populations, a one-way ANOVA test was employed to assess for statistical significance at an alpha of 0.05. Pairwise comparisons were further performed with a Tukey adjustment. All cell numbers are displayed as boxplots, which were generated by *R* 3.6.2 software.

RESULTS

Zeolite Filtration of Commercial Insulin. The porous structure of zeolite allows it to function as a molecular sieve, which can remove excipients from insulin formulations, while permitting insulin passage. The two types of zeolites evaluated were Z-Y and Mordenite. While both are aluminosilicates, they have their own unique properties.[46] Each type of aluminosilicate is capable of binding both phenol and *m*-cresol (Figure 2). However, Z-Y demonstrated a greater overall adsorption for both *m*-cresol and phenol when compared to that of mordenite (Figure 2a,b). These results are consistent with prior reports and are likely due to the 3D pore structure of Z-Y as opposed to the 2D structure found in mordenite.[46] Z-Y did not absorb insulin, as demonstrated from HPLC analysis following Z-Y passage (97.8% ± 0.6) (Figure 2c) while providing minimal removal of zinc (Figure S1). Therefore, Z-Y was chosen as the zeolite agent for subsequent *in vitro* and *in vivo* studies. In-line pressure tests revealed that pressure was directly proportional to the amount of Z-Y (Figure S2). Z-Y amounts of 40 mg or greater induced pressures at or greater than 80 psi, which were sufficient to trigger occlusion pump errors.

Cytotoxicity of Commercial Insulin and Diluents *In Vitro*: Human and Mouse Cell Lines. Mouse and human

https://doi.org/10.1021/acsptsci.1c00047
ACS Pharmacol. Transl. Sci. 2021, 4, 1161−1174

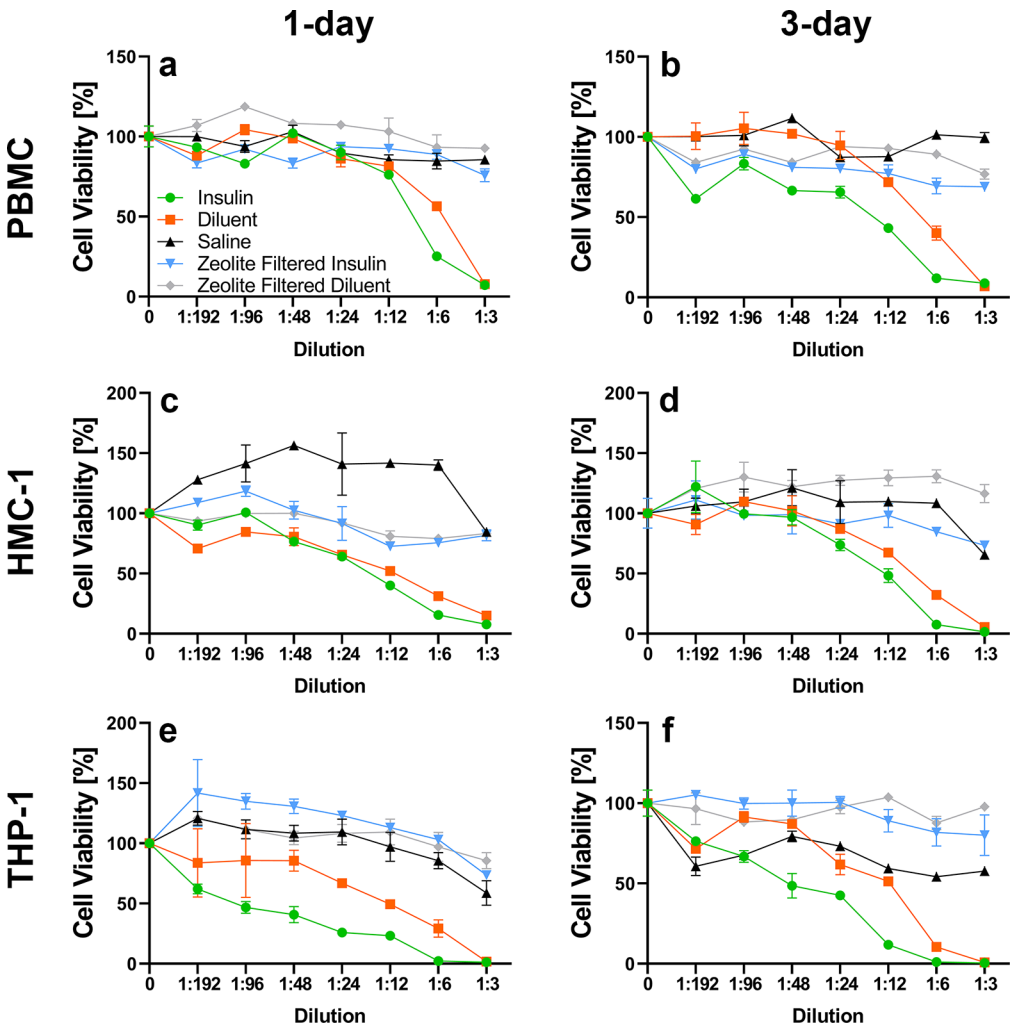

Figure 3. Human cell exposure: Saline (▲), diluent (■), insulin (●), zeolite-filtered diluent (◆), and zeolite-filtered insulin (▼). Z-Y at a concentration of 20 mg/mL used to filter Humalog U-100 diluent and Humalog U-100 Insulin showed significant differences in cell viability a high concentration of both insulin and diluent when peripheral blood mononuclear cells (PBMC) (a and b), human mast cells (HMC-1) (c and d), and human monocytes (THP-1) (e and f) were exposed for 24 and 72 h. Error bars represent standard deviation (n = 3, triplicate measurements). Diluent contains lower total PP than Humalog (2.25 and 3.15 mg/mL, respectively).

primary cells and cell lines were utilized to determine which cell types are susceptible to *m*-cresol and phenol cytotoxicity and to assess the effect of Z-Y filtration on cellular cytotoxicity (e.g., Z-Y leaching). To distinguish between insulin and excipient-derived cytotoxicity, Eli Lilly diluent containing 2.25 mg/mL *m*-cresol/phenol (no insulin protein) was administered. *In vitro* studies depicted in Figures 3 and 4 demonstrate that Z-Y filtration of both *m*-cresol and phenol from Humalog mitigated the cytotoxic effects of these excipients. Different primary cells and cell lines in both the human and mouse categories all manifested similar reactivity to *m*-cresol and phenol, which emphasizes the nonspecific cytotoxicity of these two compounds *in vitro*. A significant decrease in cell viability in 3T3-L1 cell lines was noted at a 1:6 dilution, which equates to an *m*-cresol/phenol concentration of 0.53 mg/mL in insulin samples and 0.27 mg/mL in diluent samples ($p < 0.05$). Significance across all other mouse cell lines is apparent at the 1:12 dilution, or 0.27 mg/mL of *m*-cresol/phenol in insulin samples and 0.13 mg/mL in diluent samples ($p < 0.05$) (Table S1). A decrease in cell viability for human PBMCs was noted at a 1:6 dilution, while HMC-1 and THP-1 cells showed decreases in viability at lower concentrations of 1:12 and 1:24 dilution respectively ($p < 0.05$) (Table S2). Data sets for 1 and 3 days for each respective cell line demonstrate minimal changes in cell viability implying that viability is diminished within the first 24 h of exposure. On the basis of *in vitro* findings, it was anticipated that a reduction of *m*-cresol and phenol by >80% during infusion would improve adverse tissue reaction during infusion.

Mouse Air-Pouch Model. Leukocyte influx and tissue reaction to infused saline (S), diluent (D), insulin (I), and Z-Y-filtered diluent/insulin (ZD and ZI) were assessed in the murine air-pouch model. *In vivo* experiments demonstrated a significant decrease in inflammatory cells when Humalog U-100 insulin and diluent were passed through the Z-Y filter (Figure 5). These results were analyzed using flow cytometry FACS analysis. FACS results yielded quantitative values for each inflammatory cell population present in the air pouch at the time of lavage and tissue harvest.

There was a decrease in total cell accumulation in the S, ZD, and ZI infusions compared to those in D and I infusions at 3 days ($p < 0.01$, Table 1b). No statistical differences were seen between the D- and I-infused groups (Table 1b). Cellular subgroup analysis for each infusion state was also analyzed. A

https://doi.org/10.1021/acsptsci.1c00047
ACS Pharmacol. Transl. Sci. 2021, 4, 1161−1174

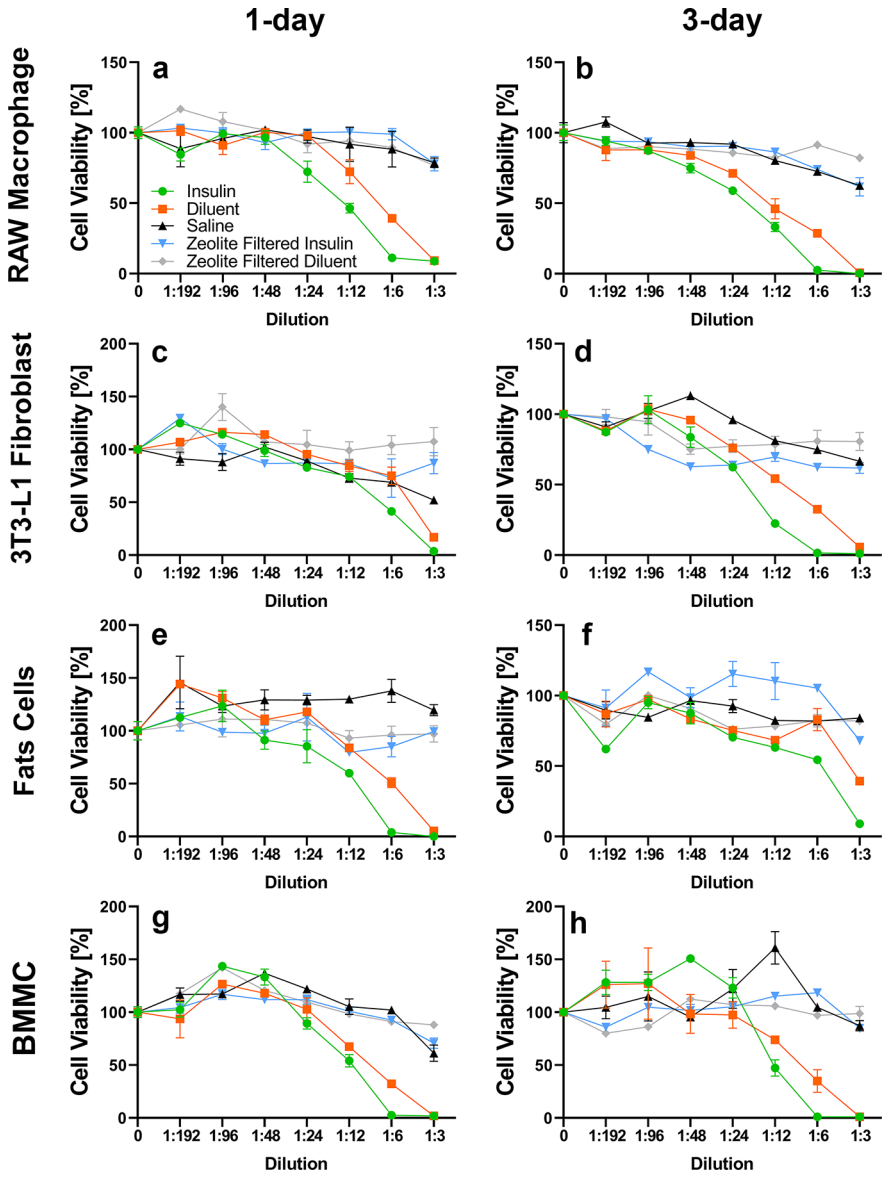

Figure 4. Mouse cell exposure: Saline (▲), diluent (■), insulin (●), zeolite-filtered diluent, (◆) zeolite-filtered insulin (▼). Zeolite Y at a concentration of 20 mg/mL used to filter Humalog U-100 diluent and Humalog U-100 insulin showed significant differences in cell viability a high concentration of both insulin and diluent when RAW macrophages (a and b), mouse fibroblast (3T3-L1) (c and d), mouse fat cells (3T3-L1 derived) (e and f), and BMMC (g and h) were exposed for 24 and 72 h. Error bars represent standard deviation (n = 3, triplicate measurements). Diluent contains lower total PP than Humalog (2.25 and 3.15 mg/mL, respectively).

one-way ANOVA demonstrated that there was no statistical difference in neutrophils in the S-infused STZ-induced diabetic mice when compared to either the D- or I-infused mice (p > 0.05, Table 1d). Tukey's post hoc analysis revealed significance in the ZD and ZI groups when compared to the D-infused group but not the I-infused group (p < 0.05, Table 1d). Macrophage/monocyte data demonstrated statistical significance in the S, ZD, and ZI infusions compared to that in the D and I infusions at 3 days, similar to the total cell data (p < 0.05, Table 1f). Lymphocyte data manifested a decrease in the S, ZD, and ZI groups when compared to the I-infused group (p < 0.01) but not the D-infused group (p > 0.05) (Table 1h).

Qualitative Evaluation of Postlavage Air-Pouch Tissue for Histopathology before and after Z-Y Treatment of Commercial Insulin and Diluent *In Vivo*. H&E, F4/80, and CD31 staining assessed the inflammatory cell accumulation in the air pouch postinfusion, as well as vascularization of the infusion site. Histological analysis revealed a reduction in inflammatory cell recruitment and a reduction in neovascularization in the Z-Y-filtered insulin compared to Humalog U-100 (Figure 5). The most significant accumulation of inflammatory cells was predominately macrophages as confirmed using F4/80 immunohistochemistry. Analysis of macrophage distribution demonstrated limited numbers of macrophages present for saline, Z-Y-filtered diluent, and Z-Y-filtered insulin infusions (Figure 6a,b,k,n). Diluent and insulin infusions showed significant accumulation of macrophages at the air pouch interface (Figure 6e,h). Neutrophils and macrophages were both present at the air-pouch interface, whereas macrophages were the predominant cell in the surrounding tissue. Analysis of blood vessel distribution demonstrated limited neovascularization present for saline, Z-Y-filtered diluent, and Z-Y-filtered insulin infusions (Figure 6c,l,o). Diluent and insulin infusions showed

https://doi.org/10.1021/acsptsci.1c00047
ACS Pharmacol. Transl. Sci. 2021, 4, 1161−1174

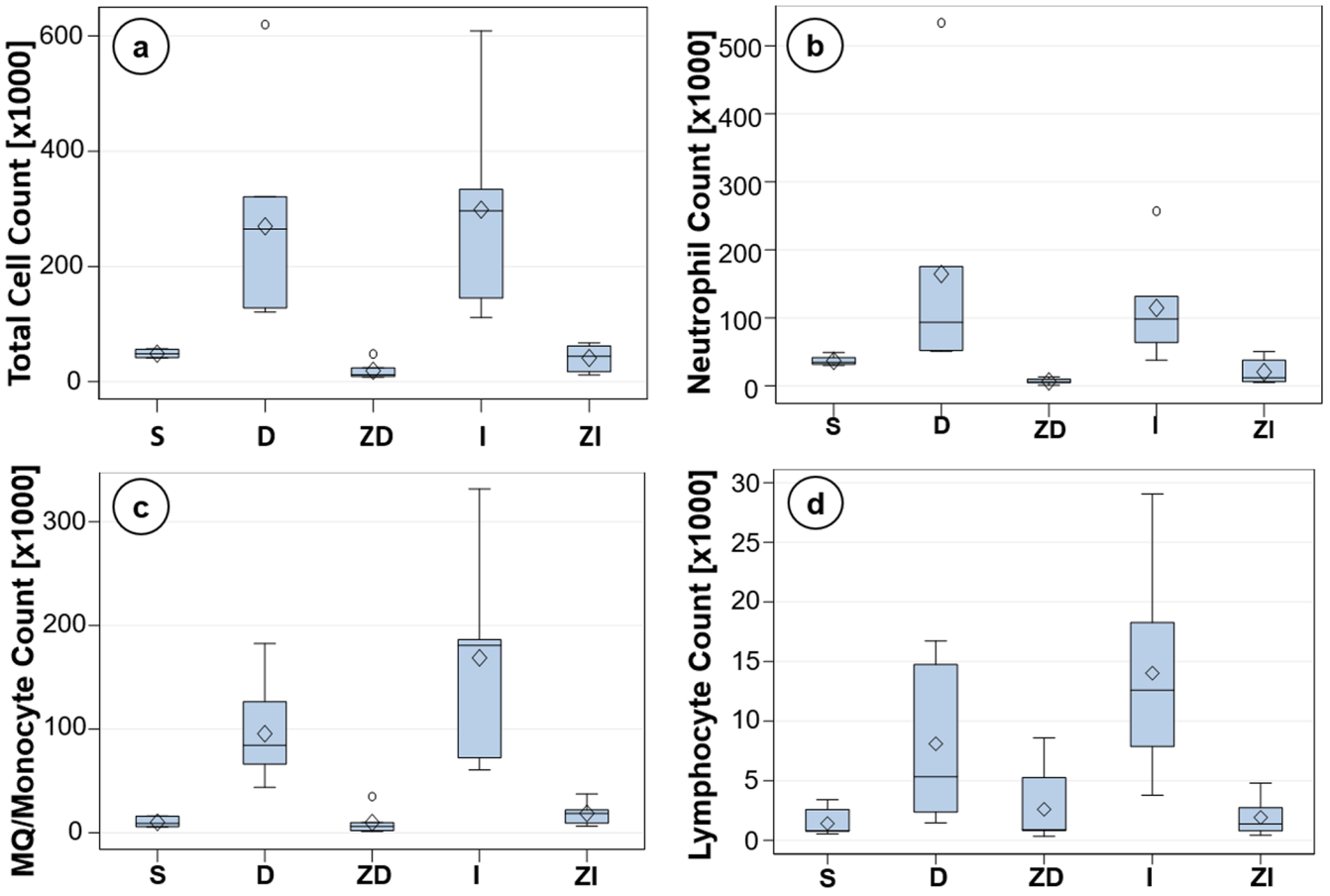

Figure 5. FACS: Cell counts via flow cytometry (FACS) analysis give quantifiable differences in the amounts of inflammatory cells present in each infusion scenario. (a) Total leukocyte counts, (b) neutrophil counts, (c) macrophage/monocyte counts, and (d) lymphocyte counts. Cell populations from saline (n = 7), filtered diluent (n = 7), and filtered insulin (n = 6) show decreased cell counts in relation to diluent (n = 7) and insulin (n = 6) in all cases.

significant vascularization in the tissue surrounding the air pouch, providing more opportunity for inflammatory cell infiltration (Figure 6f,i). Moreover, the tissue reaction to infused Z-Y-filtered diluent and insulin were equivalent or less than the saline infusion, implying that Z-Y-filtered insulin alleviates the observed inflammatory response from insulin due to lack of *m*-cresol/phenol.

Insulin Stability *In Vitro*. Crystallographic data demonstrates that PP stabilizes the insulin hexamer and, in part, prevents insulin degradation.[33] While an efficient mechanism for removal has been demonstrated, this must be balanced against protein stability. CD was used to characterize the secondary structure and oligomeric state of Humalog because of filtration through dextran-coated Z-Y. CD spectroscopy is beneficial for protein analysis as it is a nondestructive technique performed in the same pharmaceutical solution for drug delivery. An excess of Z-Y was used for filtration of Humalog for complete removal of *m*-cresol/phenol. Humalog protein was scanned first, then filtered through Z-Y, and scanned immediately after. The R6 hexamer of fast-acting insulin is evident by a negative feature around 260−250 nm.[55] Humalog in its commercially available form shows a negative feature in this region, which is lost after passing through the Z-Y filter (Figure 7 a). To determine changes in the protein's secondary structure, far-UV CD was utilized. Secondary structure spectra for Humalog and Z-Y-filtered Humalog are shown in Figure 7b. The difference between the α helix (208 and 222 nm) peaks are <1.5 mdeg, suggesting that removal of PP does not significantly alter the secondary structure of Humalog protein and that it is expected to retain its activity. To confirm insulin activity of Z-Y-filtered insulin, STZ-induced diabetic mice blood glucose averages (Figure 8, NS between Humalog and ZF-Humalog) were observed following administration of Humalog and ZF-Humalog during infusion over 3 days. Average blood glucose levels were maintained with no significant difference in total units of Humalog and Z-Y-Humalog. These data demonstrate that blood glucose levels were equally maintained over 72 h between Humalog and Z-Y-Humalog.

DISCUSSION

Infusion set failure and underlying tissue damage caused by PP could impede the progress of CSII technology.[34,35] Limited wear time accompanied by infusion site rotation are the current solutions to minimize tissue damage and maintain infusion site integrity over time.[9] These practices, while ultimately beneficial, will not allow for insulin infusion sets to perform beyond a few days. The removal of PP prior to infusion into the skin and its immediate effects on insulin protein stability in regard to insulin dwell time postfiltration are still under investigation. In our mouse studies, the dwell time is less than 1 h given the placement of the filtration apparatus (Figure 1). Nevertheless, infusion set length used in clinical settings are up to 43 in., which could result in a dwell

https://doi.org/10.1021/acsptsci.1c00047
ACS Pharmacol. Transl. Sci. 2021, 4, 1161−1174

Table 1. Statistical Analysis of Total Cell Data from the Mouse Air-Pouch Model[a]

a. Total Leukocyte Count (× 1000)

mouse status		3 days *n*	mean	standard deviation
diabetic	S	7	48.6	7.2
	D	7	269.9	173.8
	I	6	298.7	178.2
	ZD	7	19.1	14.1
	ZI	6	41.2	23.8

b. Post Hoc Multiple Comparisons (Tukey-Adjusted)

p-value		D	ZD	I	ZI
diabetic 3 days	S	<0.01	NS	<0.01	NS
	D		<0.01	NS	<0.01
	ZD			<0.001	NS
	I				<0.01

c. Neutrophil Count (× 1000)

mouse status		3 days *n*	mean	standard deviation
diabetic	S	7	36.9	6.6
	D	7	164.5	170.5
	I	6	114.6	77.7
	ZD	7	6.6	4.0
	ZI	6	20.6	19.1

d. Post Hoc Multiple Comparisons (Tukey-Adjusted)

p-value		D	ZD	I	ZI
diabetic 3 days	S	NS	NS	NS	NS
	D		<0.05	NS	<0.05
	ZD			NS	NS
	I				NS

e. Macrophage/Monocyte Count (× 1000)

mouse status		3 days *n*	mean	standard deviation
diabetic	S	7	10.1	4.3
	D	7	95.6	46.5
	I	6	168.8	96.2
	ZD	7	9.9	11.5
	ZI	6	18.7	11.2

f. Post Hoc Multiple Comparisons (Tukey-Adjusted)

p-value		D	ZD	I	ZI
diabetic 3 days	S	<0.05	NS	<.0001	NS
	D		<0.05	NS	<0 05
	ZD			<.0001	NS
	I				<.0001

g. Lymphocyte Count (× 1000)

mouse status		3 days *n*	mean	standard deviation
diabetic	S	7	1.4	1.1
	D	7	8.1	6.4
	I	6	14.0	8.9
	ZD	7	2.6	3.1
	ZI	6	1.9	1.6

h. Post Hoc Multiple Comparisons (Tukey-Adjusted)

p-value		D	ZD	I	ZI
diabetic 3 days	S	NS	NS	0.001	NS
	D		NS	NS	NS
	ZD			<0.01	NS
	I				<0.01

[a]Data represent *n*-value, mean, and standard deviation followed by statistical analysis for total leukocyte (a, b), neutrophil (c, d), macrophage/monocyte (e, f), and lymphocyte (g, h) recruitment following infusion of saline (S), diluent (D), insulin (I), zeolite-filtered insulin (ZI), and zeolite-filtered diluent (ZD) for 3 days in diabetic mice. For total cells and macrophages, there was a significant difference between zeolite-filtered and non-filtered insulin and diluent, suggesting that the removal of *m*-cresol and phenol reduced the total inflammatory response at the site of infusion.

time of 4 h at an infusion rate of 0.5 U/h.[54] Additionally, occlusion of the cannula tip has been reported after extended insulin infusion usage.[30,56,57] Therefore, it warrants further investigation if cannula tip occlusions are associated with insulin-preservative-induced inflammation. Nevertheless, the effects of PP removal on the infusion site demonstrate the possibilities of extending the useful lifespan of CSII. In the present study, we demonstrated that zeolite Y filtration effectively removes cytotoxic *m*-cresol and phenol excipients from standard insulin formulations. The resultant degree of tissue inflammation was comparable to that observed with saline injections. Thus, excipient removal has the potential to extend the longevity of insulin infusion sets by mitigating the inflammatory response. Nonetheless, as demonstrated in Figure 2, Z-Y is only capable of removing 87% of phenol and 97% of *m*-cresol at the highest Z-Y concentration assessed (80 mg/mL). Figure 2c demonstrated Z-Y coated with dextran showed negligible amounts of insulin adsorption for the tested parameters (20 mg zeolite:1 mL Humalog). Nevertheless, it might be possible that insulin adsorption will vary depending on the zeolite insulin ratio utilized. Even without 100% removal, *in vitro* data demonstrates that excipient toxicity is diminished after a 1:12 dilution (~83%) (Figures 3 and 4), indicating that cytotoxicity is negligible when most PP are removed from insulin formulations. *In vivo* data (Figures 5 and 6) further elucidate the effects of PP removal. With a statistically significant reduction in total inflammatory cells, and specifically in macrophage populations (Table 1), in-line filtration of PP resulted in an overall reduced inflammatory response. It was also noted that wound healing responses, such as increased vascularization, were seemingly reduced after removal of PP. These effects could result in reduced irritation that would extend the useful lifespan of infusion sets beyond 3 days.

Despite these *in vitro* and *in vivo* data, complete removal of *m*-cresol/phenol at the manufacturer is not a viable solution as these compounds are required for insulin protein stabilization and as an antimicrobial agent.[32,33] We observed a loss in hexameric structure with *m*-cresol/phenol removal (Figure 7) despite the retention of zinc in the formulation (Figure S2). The hexameric state is used to stabilize the protein as the monomer can degrade or form large oligomers predominated by a stacked β-sheet structure known as amyloid fibrils.[58,59] Insulin fibrils have demonstrated inflammatory effects which further reduce insulin efficacy.[39,60] Despite the changes in overall oligomeric state, we did not observe significant

https://doi.org/10.1021/acsptsci.1c00047
ACS Pharmacol. Transl. Sci. 2021, 4, 1161−1174

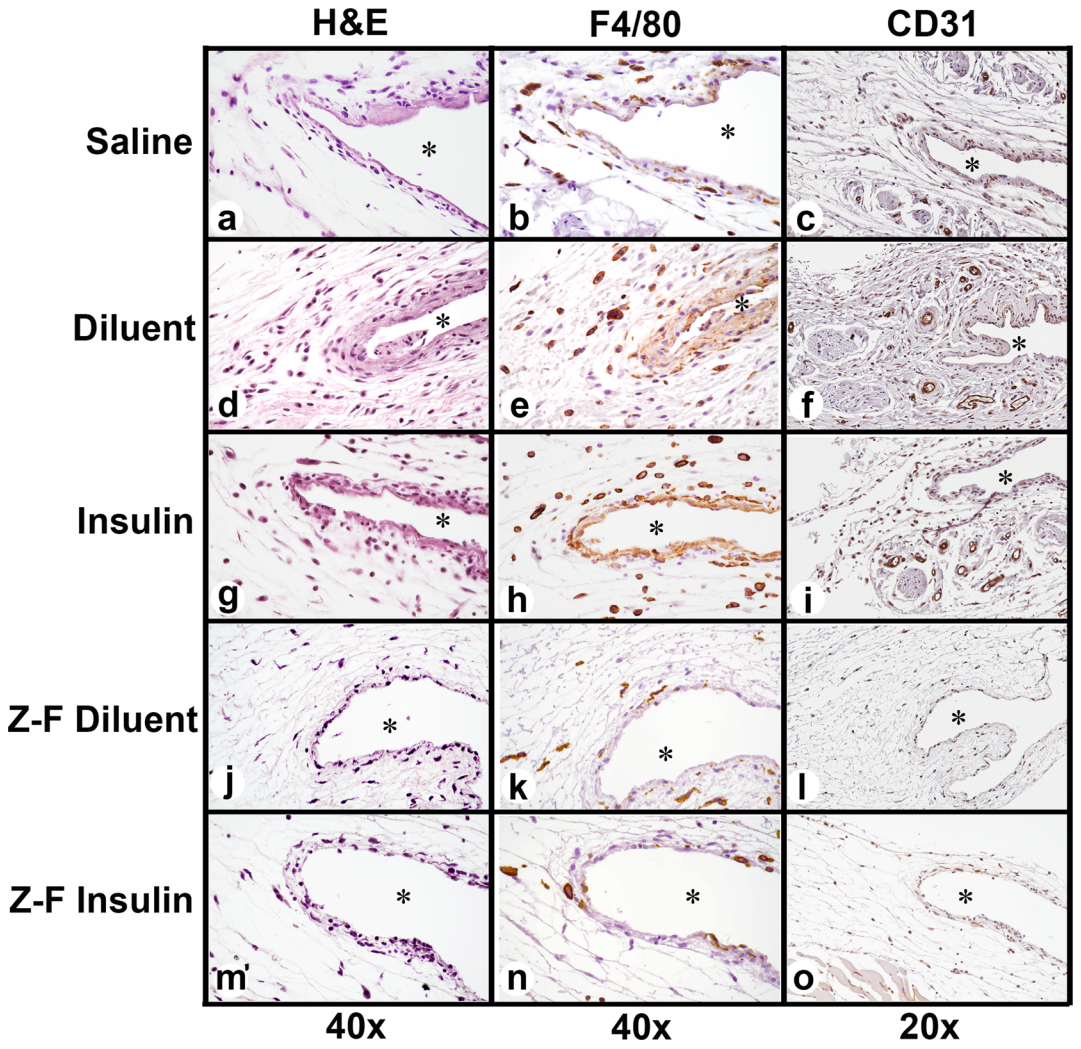

Figure 6. Air-pouch histology at 3 days of infusion: (a, d, g, j, and m) H&E staining (40×). (b, e, h, k, and n) F4/80 Macrophage stain (40×). (c, f, i, l, and o) CD31 Vascular endothelial cell stain (20×). * denotes air pouch.

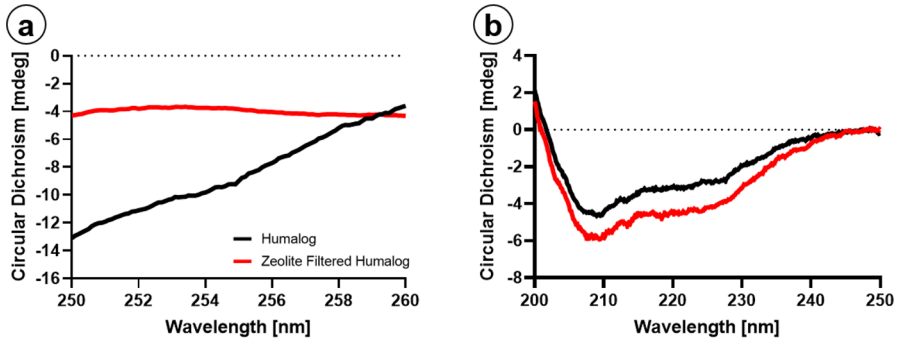

Figure 7. Protein structural analysis: (a) Humalog (black) hexamer negative peak is diminished following zeolite filtration (red). (b) Secondary structure is unaffected.

differences in the secondary structure analysis following Z-Y filtration. Near-UV CD has been used to examine tertiary structure of insulin with and without PP.[55] Size-exclusion HPLC or mass spectrometry is typically used to determine either the presence or absence of oligomerization.[32] However, CD allows for protein analysis in PP solution which otherwise complicates HPLC absorbance due to the presence of aromatics. Most importantly, our CD data revealed no observable increase in characteristic β-sheet wavelengths,[59] suggesting the filtration does not immediately produce significant amounts of insulin fibril. Furthermore, the dissociation from hexamer to monomer, which we demonstrated to occur postfiltration, is a key step in insulin absorption.[30,61] It is possible that certain pharmacokinetic parameters, T_{max}, may decrease and align more closely with endogenous insulin absorption.[62] Other considerations are dwell time for infusion sets, which vary based on tubing length and infusion rate. Considering a basal infusion rate of 0.5 U/h

https://doi.org/10.1021/acsptsci.1c00047
ACS Pharmacol. Transl. Sci. 2021, 4, 1161−1174

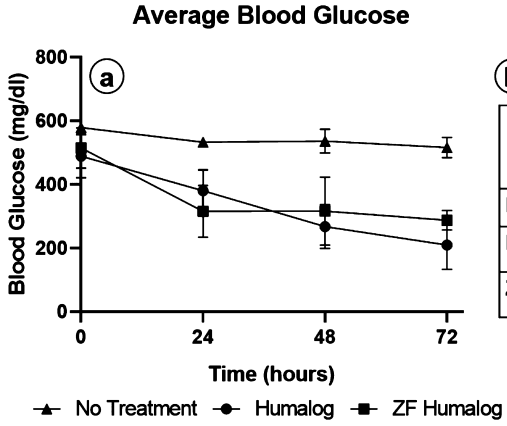

b

Treatment	Average Units of Insulin (U)
No treatment	0 U
Humalog	1.621 ± 0.547
ZF Humalog	1.592 ± 0.362

Figure 8. Blood glucose control: (a) Average blood glucose levels over the duration of infusion. (b) Average units of insulin used over the duration of infusion. Two-way Anova demonstrated average daily blood glucose for Humalog and Z-Y-filtered Humalog showed no statistical significance ($n = 6$) ($p > 0.05$) between each other, and both showed significance compared to the no insulin treatment in STZ induced diabetic mice ($n = 4$) ($p < 0.05$).

and a 43 in. tubing set, the maximum dwell time would be up to 4 h from insulin reservoir to delivery.[54] Previous studies *in vitro* have not shown fibrillation or degradation occurring at 4 h.[32,36,63,64] However, it remains to be determined how exposure to tubing and filter conditions will impact protein stability without PP over time.

Notwithstanding these conformational changes, we tested insulin activity following Z-Y filtration by infusion in chemically induced diabetic mice. Our *in vivo* results demonstrate that average blood glucose levels are equally maintained for Humalog compared to ZF-Humalog (Figure 8). To overcome protein stability challenges, we used an in-line filtration approach, wherein Humalog was passed through standard infusion tubing with Z-Y and a sterile filter built in as depicted in Figure 1d. By having the filter in line, this reduces the total dwell time of filtered Humalog in the tubing. Long-term exposure to tubing conditions could contribute to protein fibril formation or degradation. However, to translate this approach into clinical practice, further investigations into the stability and lifespan of filtered protein are warranted. Patients wearing infusion pumps could expose their insulin to a variety of conditions which could promote insulin protein aggregation, (e.g., fibril formation), through increased heat or agitation.[36,65] Therefore, an in-depth biochemical and *in vivo* activity analysis should be performed longitudinally to measure insulin fibril formation and a possible loss of biochemical protein activity at clinically relevant time points and exposure conditions postfiltration. Murine models provide the foundation to address mechanistic questions at the molecular level. Nevertheless, limitations of murine subdermal implant models are clear when compared to human skin. For example, rodent skin differs from human skin in that it lacks apocrine sweat glands and rete ridges/dermal papillae.[66] Rodent skin also presents a panniculosus carnosus layer, which produces rapid contraction after wounding, which differs from human wound healing that occurs by re-epithelialization and granulation tissue formation.[66,67] The relative lack of meaningful subcutaneous fatty tissue levels in the mouse model is an additional critical species difference and study limitation. These are all important differences to consider when evaluating infusion devices considered for human adipose-rich sites. Thus, future studies should be directed at assessing tissue reaction and insulin viability following unadulterated insulin infusion and Z-Y insulin infusion while evaluating insulin absorption and glucose variability over time in a preclinical porcine animal model, which more closely approximates human skin.

We recently demonstrated that PP, currently present in all commercially available insulin formulations, contribute to leukocyte recruitment and activation of the inflammatory cascade.[35] The present study demonstrated that the usage of in-line exchange resins, such as zeolite Y, successfully remove PP. Excipient removal prior to insulin infusion significantly reduced infusion site associated inflammation without compromising insulin functionality. This approach represents the proof of concept that in-line Z-Y PP removal assists in lowering inflammation at the site of insulin infusion and thus could lead to extending the functional lifespan of insulin infusion sets *in vivo*. Nevertheless, Z-Y might not prove to be the optimal material given its associated backpressure potentially leading to pump failure over time, its inability to remove all diluents/excipients from current insulin formations, and the loss of the insulin hexamer structure. However, given that hexameric dissociation is a rate-limiting step for rapid-acting insulin absorption, this could result in faster insulin absorption after removal of phenolic preservative, which might be a desirable outcome. Overall, these results provide a foundation for investigating other methods or materials that may overcome Z-Y limitations. Future research directed at mitigating the toxic effects of these PP/insulin-stabilizing excipients is warranted.

■ ASSOCIATED CONTENT

Supporting Information

The Supporting Information is available free of charge at https://pubs.acs.org/doi/10.1021/acsptsci.1c00047.

ICP-MS for zinc filtration, in-line pressure monitoring, and *in vitro* mouse cell and human cell statistics (PDF)

■ AUTHOR INFORMATION

Corresponding Author

Ulrike Klueh − *Department of Biomedical Engineering, Integrative Biosciences Center, Wayne State University, Detroit, Michigan 48202, United States;* orcid.org/0000-0003-1104-7704; Email: klueh@wayne.edu

https://doi.org/10.1021/acsptsci.1c00047
ACS Pharmacol. Transl. Sci. 2021, 4, 1161−1174

Authors

Adam Mulka − *Department of Biomedical Engineering, Integrative Biosciences Center, Wayne State University, Detroit, Michigan 48202, United States*

Brianne E. Lewis − *Department of Biomedical Engineering, Integrative Biosciences Center, Wayne State University, Detroit, Michigan 48202, United States*

Li Mao − *Department of Biomedical Engineering, Integrative Biosciences Center, Wayne State University, Detroit, Michigan 48202, United States*

Roshanak Sharafieh − *Department of Surgery, School of Medicine, University of Connecticut, Farmington, Connecticut 06030-2100, United States*

Shereen Kesserwan − *Department of Biomedical Engineering, Integrative Biosciences Center, Wayne State University, Detroit, Michigan 48202, United States*

Rong Wu − *Connecticut Convergence Institute, School of Medicine, University of Connecticut, Farmington, Connecticut 06030-6022, United States*

Donald L. Kreutzer − *Department of Surgery, School of Medicine, University of Connecticut, Farmington, Connecticut 06030-2100, United States*

Complete contact information is available at: https://pubs.acs.org/10.1021/acsptsci.1c00047

Notes

The authors declare the following competing financial interest(s): U.K. and D.K. are co-founders and co-owners of the small business Cell and Molecular Tissue Engineering, LLC, Avon, CT. No other potential conflicts of interest relevant to this article are present.

The raw data required to reproduce the findings regarding the *in vitro* studies and the FACS data are available as supplementary data.

■ ACKNOWLEDGMENTS

This work was supported by The Leona M. and Harry B. Helmsley Charitable Trust (2017PG-T1D008). The Microscopy, Imaging, and Cytometry Resources Core is supported, in part, by NIH Center grants P30 CA22453 to the Karmanos Cancer Institute and R50 CA251068-01 to Dr. Moin, Wayne State University, and the Perinatology Research Branch of the National Institutes of Child Health and Development. HPLC analyses were performed at the Lumigen Instrument Center, Wayne State University, Detroit, MI.

■ REFERENCES

(1) Rowley, W. R., Bezold, C., Arikan, Y., Byrne, E., and Krohe, S. (2017) Diabetes 2030: Insights from Yesterday, Today, and Future Trends. *Popul. Health Manage. 20*, 6−12.

(2) Umpierrez, G. E., and Klonoff, D. C. (2018) Diabetes Technology Update: Use of Insulin Pumps and Continuous Glucose Monitoring in the Hospital. *Diabetes Care 41* (8), 1579.

(3) Nathan, S., Genuth, S., Lachin, J., Cleary, P., Crofford, O., Davis, M., Rand, L., and Siebert, C. (1993) The effect of intensive treatment of diabetes on the development and progression of long-term complications in insulin-dependent diabetes mellitus. *N. Engl. J. Med. 329*, 977−986.

(4) Pfützner, A., Sachsenheimer, D., Grenningloh, M., Heschel, M., Walther-Johannesen, L., Gharabli, R., and Klonoff, D. (2015) Using Insulin Infusion Sets in CSII for Longer Than the Recommended Usage Time Leads to a High Risk for Adverse Events: Results From a Prospective Randomized Crossover Study. *J. Diabetes Sci. Technol. 9* (6), 1292−1298.

(5) U. S. Food and Drug Administration/Center for Drug Evaluation and Research. (2017) *Drug Approval Package: Admelog (insulin lispro)*, Application Number 209196. https://www.accessdata.fda.gov/drugsatfda_docs/nda/2017/209196Orig1s000TOC.cfm.

(6) Al Hayek, A. A., Robert, A. A., and Al Dawish, M. A. (2018) Skin-Related Complications Among Adolescents With Type 1 Diabetes Using Insulin Pump Therapy. *Clin. Med. Insights: Endocrinol. Diabetes*, DOI: 10.1177/1179551418798794.

(7) Gentile, S., Strollo, F., and Ceriello, A. (2016) Lipodystrophy in Insulin-Treated Subjects and Other Injection-Site Skin Reactions: Are We Sure Everything is Clear? *Diabetes Ther. 7* (3), 401−409.

(8) Hauzenberger, J. R., Hipszer, B. R., Loeum, C., McCue, P. A., DeStefano, M., Torjman, M. C., Kaner, M. T., Dinesen, A. R., Chervoneva, I., Pieber, T. R., and Joseph, J. I. (2017) Detailed Analysis of Insulin Absorption Variability and the Tissue Response to Continuous Subcutaneous Insulin Infusion Catheter Implantation in Swine. *Diabetes Technol. Ther. 19* (11), 641−650.

(9) Evert, A. B., Bode, B. W., Buckingham, B. A., Nardacci, E., Verderese, C. A., Wolff-McDonagh, P., Walsh, J., and Hirsch, I. B. (2016) Improving Patient Experience With Insulin Infusion Sets: Practical Guidelines and Future Directions. *Diabetes Educator 42* (4), 470−484.

(10) Frid, A. H., Kreugel, G., Grassi, G., Halimi, S., Hicks, D., Hirsch, L. J., Smith, M. J., Wellhoener, R., Bode, B. W., Hirsch, I. B., et al. (2016) New Insulin Delivery Recommendations. *Mayo Clin. Proc. 91*, 1231−1255.

(11) Patton, S. R., Eder, S., Schwab, J., and Sisson, C. M. (2010) Survey of insulin site rotation in youth with type 1 diabetes mellitus. *J. Ped. Health Care 24*, 365−371.

(12) Famulla, S., Hövelmann, U., Fischer, A., Coester, H.-V., Hermanski, L., Kaltheuner, M., Kaltheuner, L., Heinemann, L., Heise, T., and Hirsch, L. (2016) Insulin Injection Into Lipohypertrophic Tissue: Blunted and More Variable Insulin Absorption and Action and Impaired Postprandial Glucose Control. *Diabetes Care 39* (9), 1486.

(13) Deeb, A., Abdelrahman, L., Tomy, M., Suliman, S., Akle, M., Smith, M., and Strauss, K. (2019) Impact of Insulin Injection and Infusion Routines on Lipohypertrophy and Glycemic Control in Children and Adults with Diabetes. *Diabetes Ther. 10* (1), 259−267.

(14) Deng, N. A.-O., Zhang, X., Zhao, F., Wang, Y., and He, H. (2018) Prevalence of lipohypertrophy in insulin-treated diabetes patients: A systematic review and meta-analysis. *J Diabetes Investig. 9*, 536−543.

(15) Thewjitcharoen, Y. A.-O., Prasartkaew, H., Tongsumrit, P., Wongjom, S., Boonchoo, C., Butadej, S., Nakasatien, S., Karndumri, K., Veerasomboonsin, V., Krittiyawong, S., and Himathongkam, T. (2020) Prevalence, Risk Factors, and Clinical Characteristics of Lipodystrophy in Insulin-Treated Patients with Diabetes: An Old Problem in a New Era of Modern Insulin. *Diabetes, Metab. Syndr. Obes.: Targets Ther. 13*, 4609.

(16) Chowdhury, T. A., and Escudier, V. (2003) Poor glycaemic control caused by insulin induced lipohypertrophy. *BMJ 327*, 383−384.

(17) Sahasrabudhe, R. A., Limaye, T. Y., and Gokhale, V. S. (2017) Insulin Injection Site Adverse Effect in a Type 1 Diabetes Patient: An Unusual Presentation. *J. Clin. Diagn. Res. 11*, OD10−OD11.

(18) Hauner, H., Stockamp, B., and Haastert, B. (1996) Prevalence of lipohypertrophy in insulin-treated diabetic patients and predisposing factors. *Exp. Clin. Endocrinol. Diabetes 104* (02), 106−110.

(19) Dimitriadis, G., Mitrou, P., Lambadiari, V., Maratou, E., and Raptis, S. A. (2011) Insulin effects in muscle and adipose tissue. *Diabetes Res. Clin. Pract. 93*, S52−S59.

(20) Layne, J. E., Parkin, C. G., and Zisser, H. (2016) Efficacy of the Omnipod Insulin Management System on Glycemic Control in Patients With Type 1 Diabetes Previously Treated With Multiple Daily Injections or Continuous Subcutaneous Insulin Infusion. *J. Diabetes Sci. Technol. 10*, 1130−1135.

(21) Ly, T. A.-O., Layne, J. E., Huyett, L. M., Nazzaro, D., and O'Connor, J. B. (2019) Novel Bluetooth-Enabled Tubeless Insulin

Pump: Innovating Pump Therapy for Patients in the Digital Age. *J. Diabetes Sci. Technol. 13*, 20−26.
(22) Layne, J. E., Parkin, C. G., and Zisser, H. (2017) Efficacy of a Tubeless Patch Pump in Patients With Type 2 Diabetes Previously Treated With Multiple Daily Injections. *J. Diabetes Sci. Technol. 11*, 178−179.
(23) Senesh, G., Bushi, D., Neta, A., and Yodfat, O. (2010) Compatibility of insulin Lispro, Aspart, and Glulisine with the Solo MicroPump, a novel miniature insulin pump. *J. Diabetes Sci. Technol. 4*, 104−110.
(24) Leelarathna, L., and Thabit, H. (2018) The Minimed() 670g Hybrid Automated Insulin Delivery System: Setting the Right Expectations. *Endocr Pract. 24*, 698−700.
(25) Schaepelynck, P., Darmon, P., Molines, L., Jannot-Lamotte, M.F., Treglia, C., and Raccah, D. (2011) Advances in pump technology: insulin patch pumps, combined pumps and glucose sensors, and implanted pumps. *Diabetes Metab. 37*, S85−S93.
(26) Breton, M. D., Kanapka, L. G., Beck, R. W., Ekhlaspour, L., Forlenza, G. P., Cengiz, E., Schoelwer, M., Ruedy, K. J., Jost, E., Carria, L., Emory, E., Hsu, L. J., Oliveri, M., Kollman, C. C., Dokken, B. B., Weinzimer, S. A., DeBoer, M. D., Buckingham, B. A., Cherñavvsky, D., and Wadwa, R. P. (2020) A Randomized Trial of Closed-Loop Control in Children with Type 1 Diabetes. *N. Engl. J. Med. 383* (9), 836−845.
(27) Karges, B., Schwandt, A., Heidtmann, B., Kordonouri, O., Binder, E., Schierloh, U., Boettcher, C., Kapellen, T., Rosenbauer, J., and Holl, R. W. (2017) Association of Insulin Pump Therapy vs Insulin Injection Therapy With Severe Hypoglycemia, Ketoacidosis, and Glycemic Control Among Children, Adolescents, and Young Adults With Type 1 Diabetes. *JAMA 318* (14), 1358−1366.
(28) Foster, N. C., Beck, R. W., Miller, K. M., Clements, M. A., Rickels, M. R., DiMeglio, L. A., Maahs, D. M., Tamborlane, W. V., Bergenstal, R., Smith, E., Olson, B. A., and Garg, S. K. (2019) State of Type 1 Diabetes Management and Outcomes from the T1D Exchange in 2016−2018. *Diabetes Technol. Ther. 21* (2), 66−72.
(29) Juarez, D. T., Ma, C., Kumasaka, A., Shimada, R., and Davis, J. (2014) Failure to reach target glycated a1c levels among patients with diabetes who are adherent to their antidiabetic medication. *Popul Health Manag 17* (4), 218−223.
(30) Bode, B. W. (2011) Comparison of pharmacokinetic properties, physicochemical stability, and pump compatibility of 3 rapid-acting insulin analogues-aspart, lispro, and glulisine. *Endocr Pract 17* (2), 271−80.
(31) Kerr, D., Wizemann, E., Senstius, J., Zacho, M., and Ampudia-Blasco, F. J. (2013) Stability and performance of rapid-acting insulin analogs used for continuous subcutaneous insulin infusion: a systematic review. *J. Diabetes Sci. Technol. 7* (6), 1595−1606.
(32) Teska, B. M., Alarcón, J., Pettis, R. J., Randolph, T. W., and Carpenter, J. F. (2014) Effects of Phenol and meta-Cresol Depletion on Insulin Analog Stability at Physiological Temperature. *J. Pharm. Sci. 103* (8), 2255−2267.
(33) Whittingham, J. L., Edwards, D. J., Antson, A. A., Clarkson, J. M., and Dodson, G. G. (1998) Interactions of Phenol and m-Cresol in the Insulin Hexamer, and Their Effect on the Association Properties of B28 Pro → Asp Insulin Analogues. *Biochemistry 37* (33), 11516−11523.
(34) Weber, C., Kammerer, D., Streit, B., and Licht, A. H. (2015) Phenolic excipients of insulin formulations induce cell death, pro-inflammatory signaling and MCP-1 release. *Toxicol Rep 2*, 194−202.
(35) Kesserwan, S., Mulka, A., Sharafieh, R., Qiao, Y., Wu, R., Kreutzer, D. L., and Klueh, U. (2020) Advancing continuous subcutaneous insulin infusion in vivo: New insights into tissue challenges. *J. Biomed. Mater. Res., Part A*, DOI: 10.1002/jbm.a.37097.
(36) Woods, R. J., Alarcón, J., McVey, E., and Pettis, R. J. (2012) Intrinsic fibrillation of fast-acting insulin analogs. *J. Diabetes Sci. Technol. 6* (2), 265−76.
(37) Bakaysa, D. L., Radziuk, J., Havel, H. A., Brader, M. L., Li, S., Dodd, S. W., Beals, J. M., Pekar, A. H., and Brems, D. N. (1996) Physicochemical basis for the rapid time-action of LysB28ProB29-insulin: dissociation of a protein-ligand complex. *Protein Sci. 5*, 2521−2531.
(38) Swinney, M. R., Cox, A. L., Hawkins, E. D., Xue, J., Garhyan, P., Stanley, J. R. L., Sule, S. V., Adragni, K., and Michael, M. D. (2021) Insulin, Not the Preservative *m*-cresol, Instigates Loss of Infusion Site Patency Over Extended Durations of CSII in Diabetic Swine. *J. Pharm. Sci. 110*, 1418−1426.
(39) Nakamura, M., Misumi, Y., Nomura, T., Oka, W., Isoguchi, A., Kanenawa, K., Masuda, T., Yamashita, T., Inoue, Y., Ando, Y., and Ueda, M. (2019) Extreme Adhesion Activity of Amyloid Fibrils Induces Subcutaneous Insulin Resistance. *Diabetes 68* (3), 609.
(40) Nilsson, M. R. (2016) Insulin amyloid at injection sites of patients with diabetes. *Amyloid 23* (3), 139−147.
(41) Shirahama, T., Miura, K., Ju, S. T., Kisilevsky, R., Gruys, E., and Cohen, A. S. (1990) Amyloid enhancing factor-loaded macrophages in amyloid fibril formation. *Lab Invest. 62*, 61−68.
(42) Eisler, G., Kastner, J. R., Torjman, M. C., Khalf, A., Diaz, D., Dinesen, A. R., Loeum, C., Thakur, M. L., Strasma, P., and Joseph, J. I. (2019) In vivo investigation of the tissue response to commercial Teflon insulin infusion sets in large swine for 14 days: the effect of angle of insertion on tissue histology and insulin spread within the subcutaneous tissue. *BMJ. Open Diabetes Res. Care 7* (1), No. e000881.
(43) Hauzenberger, J. R., Münzker, J., Kotzbeck, P., Asslaber, M., Bubalo, V., Joseph, J. I., and Pieber, T. R. (2018) Systematic in vivo evaluation of the time-dependent inflammatory response to steel and Teflon insulin infusion catheters. *Sci. Rep. 8* (1), 1132−1132.
(44) Patel, P. J., Benasi, K., Ferrari, G., Evans, M. G., Shanmugham, S., Wilson, D. M., and Buckingham, B. A. (2014) Randomized trial of infusion set function: steel versus Teflon. *Diabetes Technol. Ther. 16* (1), 15−9.
(45) Weber, C., Kammerer, D., Streit, B., and Licht, A. H. (2015) Phenolic excipients of insulin formulations induce cell death, pro-inflammatory signaling and MCP-1 release. *Toxicology Reports 2*, 194−202.
(46) Eriksson, H. (1998) Removal of toxic preservatives in pharmaceutical preparations of insulin by the use of ultra-stable zeolite Y. *Biotechnol. Tech. 12* (4), 329−334.
(47) Khalid, M., Joly, G., Renaud, A., and Magnoux, P. (2004) Removal of Phenol from Water by Adsorption Using Zeolites. *Ind. Eng. Chem. Res. 43* (17), 5275−5280.
(48) Pan, M., Omar, H. M., and Rohani, S. (2017) Application of Nanosize Zeolite Molecular Sieves for Medical Oxygen Concentration. *Nanomaterials 7*, 195.
(49) Madsen, L., Petersen, R. K., Sørensen, M.B., Jørgensen, C., Hallenborg, P., Pridal, L., Fleckner, J., Amri, E. Z., Krieg, P., and Furstenberger, G. (2003) Adipocyte differentiation of 3T3-L1 preadipocytes is dependent on lipoxygenase activity during the initial stages of the differentiation process. *Biochem. J. 375*, 539−549.
(50) Klueh, U., Kaur, M., Qiao, Y., and Kreutzer, D. L. (2010) Critical role of tissue mast cells in controlling long-term glucose sensor function in vivo. *Biomaterials 31*, 4540−4551.
(51) International Conference on Harmonisation of Technical Requirements for Registration of Pharmaceuticals for Human Use. (2005). *Validation of Analytical Procedures: Text and Methodology Q2(R1)*, ICH Secretariat, Geneva, Switzerland.
(52) Pandyarajan, V., Phillips, N. B., Rege, N., Lawrence, M. C., Whittaker, J., and Weiss, M. A. (2016) Contribution of TyrB26 to the Function and Stability of Insulin: STRUCTURE-ACTIVITY RELATIONSHIPS AT A CONSERVED HORMONE-RECEPTOR INTERFACE. *J. Biol. Chem. 291* (25), 12978−90.
(53) Wu, K. K., and Huan, Y. (2008) Streptozotocin-induced diabetic models in mice and rats. *Curr. Protoc Pharmacol. 40*, 5.47.1−5.47.14.
(54) El-Khatib, F. H., Jiang, J., and Damiano, E. R. (2009) A feasibility study of bihormonal closed-loop blood glucose control using dual subcutaneous infusion of insulin and glucagon in ambulatory diabetic swine. *J. Diabetes Sci. Technol. 3*, 789−803.

(55) Gast, K., Schüler, A., Wolff, M., Thalhammer, A., Berchtold, H., Nagel, N., Lenherr, G., Hauck, G., and Seckler, R. (2017) Rapid-Acting and Human Insulins: Hexamer Dissociation Kinetics upon Dilution of the Pharmaceutical Formulation. *Pharm. Res. 34* (11), 2270−2286.
(56) Schmid, V., Hohberg, C., Borchert, M., Forst, T., and Pfützner, A. (2010) Pilot study for assessment of optimal frequency for changing catheters in insulin pump therapy-trouble starts on day 3. *J. Diabetes Sci. Technol. 4* (4), 976−982.
(57) Kerr, D., Morton, J., Whately-Smith, C., Everett, J., and Begley, J. P. (2008) Laboratory-based non-clinical comparison of occlusion rates using three rapid-acting insulin analogs in continuous subcutaneous insulin infusion catheters using low flow rates. *J. Diabetes Sci. Technol. 2* (3), 450−455.
(58) Choi, J. H., May, B. C. H., Wille, H., and Cohen, F. E. (2009) Molecular modeling of the misfolded insulin subunit and amyloid fibril. *Biophys. J. 97* (12), 3187−3195.
(59) Ivanova, M. I., Sievers, S. A., Sawaya, M. R., Wall, J. S., and Eisenberg, D. (2009) Molecular basis for insulin fibril assembly. *Proc. Natl. Acad. Sci. U. S. A. 106* (45), 18990−18995.
(60) Iwaya, K., Zako, T., Fukunaga, J., Sörgjerd, K. M., Ogata, K., Kogure, K., Kosano, H., Noritake, M., Maeda, M., Ando, Y., Katsura, Y., and Nagase, T. (2019) Toxicity of insulin-derived amyloidosis: a case report. *BMC Endocr. Disord. 19* (1), 61.
(61) Brange, J., Owens, D. R., Kang, S., and Vølund, A. (1990) Monomeric insulins and their experimental and clinical implications. *Diabetes Care 13*, 923−954.
(62) Mann, J. L., Maikawa, C. L., Smith, A. A. A., Grosskopf, A. K., Baker, S. W., Roth, G. A., Meis, C. M., Gale, E. C., Liong, C. S., Correa, S., Chan, D., Stapleton, L. M., Yu, A. C., Muir, B., Howard, S., Postma, A., and Appel, E. A. (2020) An ultrafast insulin formulation enabled by high-throughput screening of engineered polymeric excipients. *Sci. Transl. Med. 12* (550), No. eaba6676.
(63) Zhou, C., Qi, W., Lewis, E. N., and Carpenter, J. F. (2016) Characterization of Sizes of Aggregates of Insulin Analogs and the Conformations of the Constituent Protein Molecules: A Concomitant Dynamic Light Scattering and Raman Spectroscopy Study. *J. Pharm. Sci. 105*, 551−558.
(64) Ohno, Y., Seki, T., Kojima, Y., Miki, R., Egawa, Y., Hosoya, O., Kasono, K., and Seki, T. (2019) Investigation of factors that cause insulin precipitation and/or amyloid formation in insulin formulations. *J. Pharm. Health Care Sci. 5*, 22.
(65) Iannuzzi, C., Borriello, M., Portaccio, M., Irace, G., and Sirangelo, I. (2017) Insights into Insulin Fibril Assembly at Physiological and Acidic pH and Related Amyloid Intrinsic Fluorescence. *Int. J. Mol. Sci. 18* (12), 2551.
(66) Zomer, H. D., and Trentin, A. G. (2018) Skin wound healing in humans and mice: Challenges in translational research. *J. Dermatol. Sci. 90*, 3−12.
(67) Gerber, P. A., Buhren, B. A., Schrumpf, H., Homey, B., Zlotnik, A., and Hevezi, P. (2014) The top skin-associated genes: a comparative analysis of human and mouse skin transcriptomes. *Biol. Chem. 395*, 577−591.

https://doi.org/10.1021/acsptsci.1c00047
ACS Pharmacol. Transl. Sci. 2021, 4, 1161−1174